Original Article

Improved Stability for Ring Configured MG System with FOPI-GA Method

Rasheed Abdulkader [1,*] and Abdelhamid Djari[2]

[1]Department of Electrical Engineering, Imam Mohammad Ibn Saud Islamic University (IMSIU), Riyadh, Saudi Arabia; rmabdulkader@imamu.edu.sa
[2]Department of Electrical Engineering, Echahid Cheikh Larbi Tebessi University, Tebessa, Algeria; abdelhamid.djari@univ-tebessa.dz

https://imamjournals.org/index.php/joas/issue/view/455

Abstract With the continuous expansion of distributed energy resources, microgrid (MG) systems are becoming increasingly vital to enhance the reliability and flexibility of modern power networks. However, as the number of interconnected AC–AC converters grows, the overall system dynamics become more complex, often leading to voltage instability and degraded performance. This study addresses these challenges by proposing a fractional-order control strategy aimed at improving voltage stability in interconnected MG structures. The research focuses on developing and evaluating a non-integer PI controller designed to enhance system robustness and transient response. To this end, the MG model incorporating multiple converters is first linearized and simulated within the Matlab/Simulink environment. The results demonstrate that the proposed fractional-order PI controller significantly improves dynamic performance compared to the conventional integer-order PI controller. Specifically, the simulations reveal a reduction of approximately 22% in voltage overshoot and an 18% decrease in settling time, highlighting the controller's effectiveness in maintaining stable voltage regulation under varying operating conditions. These findings confirm that the fractional-order approach offers a promising and more flexible solution for achieving enhanced stability and control

Keywords: Fractional order control; Microgrid; renewable energy; stability.

Address for correspondence:.
E-mail: rmabdulkader@imamu.edu.sa.
Received: 11.03.2025; **Revision:** 10.10.2025; **Accepted:** 30.10.2025;
Published: 02.12.2025

1. Introduction

In recent years, the utilization of renewable resources at the distribution level has become a focal point for utilities globally, offering a promising solution to the escalating cost of fossil fuels. The creation of microgrids through distributed generation systems is instrumental in the efficient use of energy resources and can significantly enhance the stability of the public power grid [1]. While this trend brings many advantages, it also introduces numerous challenges associated with distributed generation that must be addressed. Therefore, ensuring the regulation and stability of the system has emerged as a vital concern, and it forms the central objective of this paper [2].

Nowadays, as different distributed energy topologies are being explored for integrating microgrids with the national grid, the practice of using interconnected power electronic converters has been found to cause power flow reversals in the power system [3]. The incorporation of distributed generation into the main power grid might lead to bidirectional power flows,

creating disruptions in both the process and design of voltage regulation and stability [3]. This paper puts forth a control strategy, drawing upon statistical data from solar PV sources, to construct a network aimed at stabilizing and regulating a cascaded multi-converter microgrid system. To enhance the system's stability and control, a fractional order control is employed within the microgrid, designed around the 6MVA testbed at the National Center for Reliable Electric Power Transmission (NCREPT), located at the Arkansas Research and Technology Park [4].

In literature several types of control methods has been applied in order to ensure the stability of microgrid systems. Traditional proportional-internal (PI) controllers are popular due to their straightforward design process and their capability to manage the output voltage of voltage source converters (VSC). However, architectures based on PI controller loops often struggle to effectively mitigate disturbances in

large interconnected systems, such as those found in MG systems. Moreover, this kind of controller can be vulnerable to changes in parameters and operating conditions [5].

Further,control has been examined for sudden load variation in MG system in [6], while this type of controller can be computationally intensive in particular for the larger microgrid structures with several interrelated components. However, Also, sliding mode control (SMC) can obtain a high level of robustness to regulate the voltage levels of MG structures, while one significant concern with SMC is the occurrence of chattering, a phenomenon that might cause electromagnetic interference due to the rapid switching within power electronic converters [7]. Also, neural networks are also employed in [8].

Recent studies in renewable energy systems, particularly in wind energy conversion systems (WECS), have also highlighted the growing importance of fractional-order control strategies. For instance, works such as "Exploring the Potential of Hybrid Excitation Synchronous Generators in Wind Energy: A Comprehensive Analysis and Overview" [9] and "Harnessing the Potential of High-Efficiency Synchronous Generators in Wind Energy Conversion Systems" [10] have examined advanced generator topologies and their control implications. Similarly, "Advanced Modeling and Control of Wind Conversion Systems Based on Hybrid Generators Using Fractional Order Controllers" [11] and "Investigation of the Robust Fractional Order Control Approach Associated with the Online Analytic Unity Magnitude Shaper: The Case of Wind Energy Systems" [12] demonstrated the superior robustness and adaptability of fractional-order controllers compared to classical ones. Moreover, fractional-order strategies have also proven effective beyond power generation, such as in electric vehicle speed tracking [13].
This paper develops a non-integer control technique applied to a MG structure. At present, limited studies of non-integer control approaches in power structures exist, although this technique has demonstrated enormous potential in other fields. The basis of fractional calculus (FC) is well founded. Several studies indicated the advantages of non-integer order techniques for controlling and modeling the system in contract to classical inter-order control systems. Thus, these studies indicate the benefits of applying the fractional controller, which adds additional tunning parameters to the control system and results in improving the overall dynamical system, reducing sensitivity to parameter variation and minimizing the system steady state errors [14].

To address these issues, this study proposes a Fractional-Order Proportional–Integral (FOPI) controller tuned using a Genetic Algorithm (GA) to enhance voltage stability and transient performance in a ring-configured microgrid. The proposed approach builds upon the advantages of fractional-order control theory, which extends classical integer-order control by introducing an additional fractional parameter, thereby offering more flexibility in shaping system dynamics. Compared with conventional PI controllers, the FOPI controller can achieve improved damping, reduced overshoot, and enhanced robustness under varying operating conditions. The GA-based tuning further enables a global optimization of the controller parameters, ensuring optimal performance even under nonlinear and time-varying conditions.

The novel contribution of this work lies in combining the FOPI controller with GA-based tuning specifically for a multi-converter, ring-structured microgrid—an application that has not been extensively explored in existing studies. Unlike prior research focused primarily on single-converter or radial microgrid configurations, this paper emphasizes the dynamic interactions between converters in a closed-loop ring structure and demonstrates how the fractional-order design improves stability and voltage regulation across thenetwork.

Despite these advances, several performance gaps remain. Most existing fractional-order applications in renewable systems are limited to isolated generator control or simplified configurations and do not address the complex coupling and voltage interaction phenomena present in interconnected microgrids. Additionally, challenges related to parameter tuning and scalability under varying load and network conditions are often overlooked. The present study aims to bridge these gaps by extending the use of fractional-order control to a ring-based multi-converter microgrid, demonstrating through simulation that the proposed GA-optimized FOPI controller achieves faster settling time, reduced overshoot, and improved

steady-state accuracy compared with both conventional PI and existing fractional approaches.

Therefore, this work contributes not only to advancing fractional-order control applications in distributed generation systems but also provides new insights into the stabilization of complex microgrid architectures. The results presented in this paper underscore the potential of fractional calculus–based control to enhance voltage stability, robustness, and dynamic performance in modern, interconnected energy systems.

2. MG System overview

2.1. Kinematics

The development of the controller centers on an AC microgrid capable of providing power to a small town or industrial park as demonstrated in [4]. To incorporate a photovoltaic (PV) source and two load centers into a ring configuration, certain modifications are carried out, as depicted in Figure 1. This particular topology enhances reliability; if either transformer T_3 or T_4 fails or is out of service, both loads can still be powered through the precise control of two back-to-back converters, while minimizing reactive power drawn from the utility grid. Additionally, frequency control can be implemented at the
variable voltage variable frequency (VVVF) converter, and an LC filter is employed to diminish harmonics on either side of each back-to-back converter

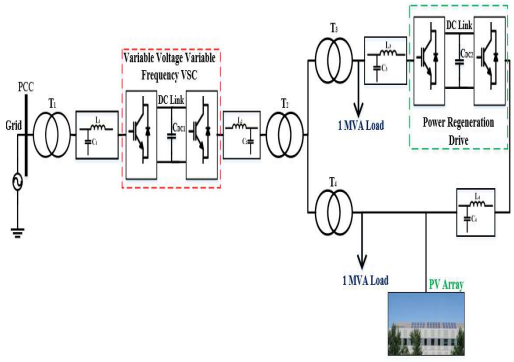

Figure 1. Cascaded converter based microgrid system.

The back to back converter topology is shown in Figure 2, which employed for both the regenerative and variable voltage variable frequency drives, further illustrating the system's complexity and innovative design. While, the system three transformers are arranged in a delta configuration, which provides a junction for a potential expansion allowing for the integration of an additional microgrid. This design also serves as an access point and with the correct setup of the delta-wye transformers, can isolate harmonics, thereby enhancing the stability and efficiency of the overall system model [15].

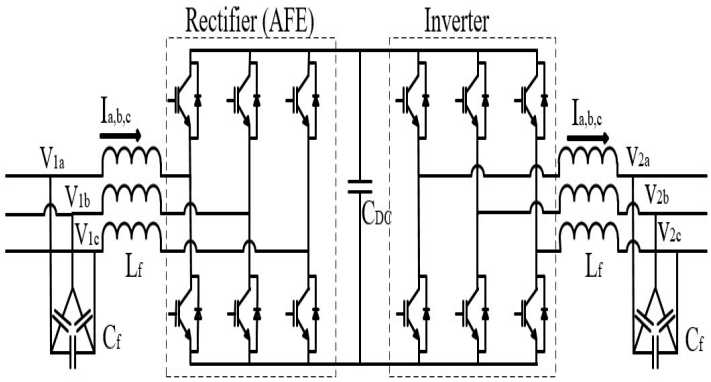

Figure 2. Regenerative and VVVF back-to-back topology.

Figure 3 presents the per-phase equivalent circuit (with capacitor values changes from delta to wye) for the microgrid system. This depiction is employed to extract the state space equations and formulate the mathematical model. The model, in turn, is utilized to craft feedback control mechanism, specifically aimed at stabilizing the microgrid when subjected to fluctuating load conditions [15].

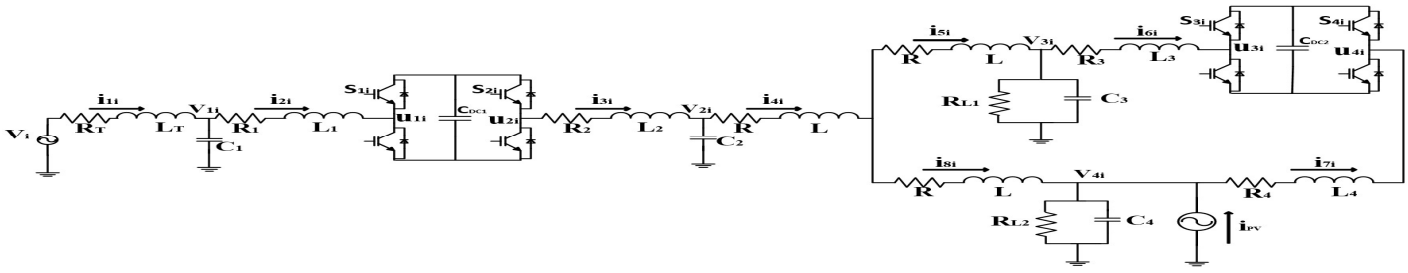

Figure 3. Single-phase equivalent circuit.

The conversion of the resulting time-varying sinusoidal variables from a three-phase coordinate system to a two-coordinate synchronous rotating frame gives rise to the mathematical model defined by the accompanying system of equations as presented in [4]. Even though transitioning to the two-coordinate synchronous frame simplifies the development of the controller compared to the original three-phase coordinates, the nonlinearity of the model still presents complexities. The issues related to variables' dependence on time-varying switching functions can be addressed through a process of linearization, as documented in [16].

Utilizing a decentralized control strategy provides several advantages over a centralized approach. A key disadvantage of the centralized method is its reliance on global data to transmit power references to the sources. This is essential so that each source can concurrently generate an appropriate response to maintain the stability of the MG (Microgrid) system. Such a strategy becomes sensitive and highly complex, especially when there is a failure within the structure.

In contrast, the decentralized methodology focuses on individual converter interfaces, which are able to recognize local state variables. This approach not only ensures the global stability of the structure but also makes the overall system more robust. By enhancing resilience and flexibility within the MG structure, the decentralized method offers a promising solution to the intricate challenges presented by centralized control [17].

2.2. Dynamics

The dynamic model has been obtained for the dynamic using Figure 3 and since the three-phase system is assumed balanced, only one phase can be taken into consideration, thus the geometrical projection onto the d_q axis gives [15]:

$$\begin{cases} \frac{dx_d}{dt} = cos\,\omega t\ \frac{dx_a}{dt} - \omega\, x_q \\ \frac{dx_q}{dt} = sin\,\omega t\ \frac{dx_a}{dt} + \omega\, x_d \end{cases}$$

(1)With nodal analysis, the set of equations below are obtained from Figure 3 as follows:$L_T \frac{di_{1i}}{dt} = -R_T i_{1i} - v_{1i} + v_i$ (2)

$$L_1 \frac{di_{2i}}{dt} = -R_1 i_{2i} - u_{1i} + v_{1i} \quad (3)$$

$$L_2 \frac{di_{3i}}{dt} = -R_2 i_{3i} + u_{2i} - v_{2i} \quad (4)$$

$$3L \frac{di_{4i}}{dt} = -3R i_{4i} + 2v_{2i} - v_{3i} - v_{4i} \quad (5)$$

$$3L \frac{di_{5i}}{dt} = -3R i_{5i} + v_{2i} - 2v_{3i} + v_{4i} \quad (6)$$

$$L_3 \frac{di_{6i}}{dt} = -R_3 i_{6i} - u_{3i} + v_{3i} \quad (7)$$

$$L_4 \frac{di_{7i}}{dt} = -R_4 i_{7i} + u_{4i} - v_{4i} \quad (8)$$

$$C_{DC1} \frac{dv_{DC}}{dt} = \sum_{i=a,b,c} \mu_{1i} i_{2i} - \sum_{i=a,b,c} \mu_{2i} i_{3i} \quad (9)$$

$$C_{DC2} \frac{dv_{DC2}}{dt} \sum_{i=a,b,c} \mu_{3i} i_{6i} - \sum_{i=a,b,c} \mu_{4i} i_{7i} \quad (10)$$

$$C_1 \frac{dv_{1i}}{dt} = i_{1i} - i_{2i} \quad (11)$$

$$C_2 \frac{dv_{2i}}{dt} = i_{3i} - i_{4i} \quad (12)$$

$$C_3 \frac{dv_{3i}}{dt} = i_{5i} - i_{6i} - \frac{v_{3i}}{R_{L1}} \quad (13)$$

$$C_4 \frac{dv_{4i}}{dt} = i_{4i} - i_{5i} + i_{7i} - \frac{v_{4i}}{R_{L2}} \quad (14)$$

$$i_{8i} = i_{5i} - i_{4i} \quad (15)$$

Where the subscript $i = a, b,$ or c. And the capacitor values are changed from the delta to wye values. Thus, Equation (1) and equations (2-15), (16- 29) are obtained, where these systems of equations are not linear since some of the state variables derivatives depend on the product of the duty functions and the state variable both of which are time-variant. Hence the non-linear model can be approximated by the first order terms of Taylor series expansion, and thus the MG system of equations can be linearized for the development of the controller implemented in this study.

The variables dependence on time-varying switching functions can be solved through linearization of the first-order terms on series expansion around the equilibrium point ($\bar{x}, \bar{u}, \bar{u}_d$). In this representation, $\bar{x}$ is the state variable vector, $\bar{u}$ is the controlled input vector and $\bar{u}_d$ is the disturbance input vector. The state space form in equations (30) and (31) represents the linearized MG system parameter values in [15]. Thus, the system become a 24th order system, where the a controller is method is designed and implemented for the higher order system to regulate the DC-link and node voltages for the MG structure.

$$\dot{d}\begin{bmatrix} i_{1d} \\ i_{1q} \end{bmatrix} = \frac{1}{L_T}\begin{bmatrix} -R_T & \omega L_T \\ -\omega L_T & -R_T \end{bmatrix}\begin{bmatrix} i_{1d} \\ i_{1q} \end{bmatrix} - \frac{1}{L_T}\begin{bmatrix} v_{1d} \\ v_{1q} \end{bmatrix} + \frac{1}{L_T}\begin{bmatrix} v_d \\ v_q \end{bmatrix} \quad (16)$$

$$\dot{d}\begin{bmatrix} i_{2d} \\ i_{2q} \end{bmatrix} = \frac{1}{L_1}\begin{bmatrix} -R_1 & \omega L_1 \\ -\omega L_1 & -R_1 \end{bmatrix}\begin{bmatrix} i_{2d} \\ i_{2q} \end{bmatrix} - \frac{v_{Cdc1}}{L_1}\begin{bmatrix} \mu_{1d} \\ \mu_{1q} \end{bmatrix} + \frac{1}{L_1}\begin{bmatrix} v_{1d} \\ v_{1q} \end{bmatrix} \quad (17)$$

$$\dot{d}\begin{bmatrix} i_{3d} \\ i_{3q} \end{bmatrix} = \frac{1}{L_2}\begin{bmatrix} -R_2 & \omega L_2 \\ -\omega L_2 & -R_2 \end{bmatrix}\begin{bmatrix} i_{3d} \\ i_{3q} \end{bmatrix} + \frac{v_{Cdc1}}{L_2}\begin{bmatrix} \mu_{2d} \\ \mu_{2q} \end{bmatrix} - \frac{1}{L_2}\begin{bmatrix} v_{2d} \\ v_{2q} \end{bmatrix} \quad (18)$$

$$\dot{d}\begin{bmatrix} i_{4d} \\ i_{4q} \end{bmatrix} = \frac{1}{L}\begin{bmatrix} -R & \omega L \\ -\omega L & -R \end{bmatrix}\begin{bmatrix} i_{4d} \\ i_{4q} \end{bmatrix} + \frac{2}{3L}\begin{bmatrix} v_{2d} \\ v_{2q} \end{bmatrix} - \frac{1}{3L}\begin{bmatrix} v_{3d} \\ v_{3q} \end{bmatrix} - \frac{1}{3L}\begin{bmatrix} v_{4d} \\ v_{4q} \end{bmatrix} \quad (19)$$

$$\dot{d}\begin{bmatrix} i_{5d} \\ i_{5q} \end{bmatrix} = \frac{1}{L}\begin{bmatrix} -R & \omega L \\ -\omega L & -R \end{bmatrix}\begin{bmatrix} i_{5d} \\ i_{5q} \end{bmatrix} + \frac{1}{3L}\begin{bmatrix} v_{2d} \\ v_{2q} \end{bmatrix} - \frac{2}{3L}\begin{bmatrix} v_{3d} \\ v_{3q} \end{bmatrix} + \frac{1}{3L}\begin{bmatrix} v_{4d} \\ v_{4q} \end{bmatrix} \quad (20)$$

$$\dot{d}\begin{bmatrix} i_{6d} \\ i_{6q} \end{bmatrix} = \frac{1}{L_3}\begin{bmatrix} -R_3 & \omega L_3 \\ -\omega L_3 & -R_3 \end{bmatrix}\begin{bmatrix} i_{6d} \\ i_{6q} \end{bmatrix} - \frac{v_{Cdc2}}{L_3}\begin{bmatrix} \mu_{3d} \\ \mu_{3q} \end{bmatrix} + \frac{1}{L_3}\begin{bmatrix} v_{3d} \\ v_{3q} \end{bmatrix} \quad (21)$$

$$\dot{d}\begin{bmatrix} i_{7d} \\ i_{7q} \end{bmatrix} = \frac{1}{L_4}\begin{bmatrix} -R_4 & \omega L_4 \\ -\omega L_4 & -R_4 \end{bmatrix}\begin{bmatrix} i_{7d} \\ i_{7q} \end{bmatrix} + \frac{v_{Cdc2}}{L_4}\begin{bmatrix} \mu_{4d} \\ \mu_{4q} \end{bmatrix} - \frac{1}{L_4}\begin{bmatrix} v_{4d} \\ v_{4q} \end{bmatrix} \quad (22)$$

$$\dot{v_{CDC1}} = \frac{1}{C_{DC}}\Big((\mu_{1d}i_{2d} + \mu_{1q}i_{2q}) - (\mu_{2d}i_{3d} + \mu_{2q}i_{3q})\Big) \quad (23)$$

$$\dot{v_{CDC2}} = \frac{1}{C_{DC}}\Big((\mu_{3d}i_{6d} + \mu_{3q}i_{6q}) - (\mu_{4d}i_{7d} + \mu_{4q}i_{7q})\Big) \quad (24)$$

$$\dot{d}\begin{bmatrix} v_{1d} \\ v_{1q} \end{bmatrix} = \frac{1}{C_1}\begin{bmatrix} i_{1d} \\ i_{1q} \end{bmatrix} - \frac{1}{C_1}\begin{bmatrix} i_{2d} \\ i_{2q} \end{bmatrix} + \begin{bmatrix} 0 & \omega \\ -\omega & 0 \end{bmatrix}\begin{bmatrix} v_{1d} \\ v_{1q} \end{bmatrix} \quad (25)$$

$$\dot{d}\begin{bmatrix} v_{2d} \\ v_{2q} \end{bmatrix} = \frac{1}{C_2}\begin{bmatrix} i_{3d} \\ i_{3q} \end{bmatrix} - \frac{1}{C_2}\begin{bmatrix} i_{4d} \\ i_{4q} \end{bmatrix} + \begin{bmatrix} 0 & \omega \\ -\omega & 0 \end{bmatrix}\begin{bmatrix} v_{2d} \\ v_{2q} \end{bmatrix} \quad (26)$$

$$\dot{d}\begin{bmatrix} v_{3d} \\ v_{3q} \end{bmatrix} = \frac{1}{C_3}\begin{bmatrix} i_{5d} \\ i_{5q} \end{bmatrix} - \frac{1}{C_3}\begin{bmatrix} i_{6d} \\ i_{6q} \end{bmatrix} + \frac{1}{R_{L1}C_3}\begin{bmatrix} -1 & \omega R_{L1}C_3 \\ -\omega R_{L1}C_3 & -1 \end{bmatrix}\begin{bmatrix} v_{3d} \\ v_{3q} \end{bmatrix} \quad (27)$$

$$\dot{d}\begin{bmatrix} v_{4d} \\ v_{4q} \end{bmatrix} = \frac{1}{C_4}\left(\begin{bmatrix} i_{4d} \\ i_{4q} \end{bmatrix} - \begin{bmatrix} i_{5d} \\ i_{5q} \end{bmatrix} + \begin{bmatrix} i_{7d} \\ i_{7q} \end{bmatrix}\right) + \frac{1}{R_{L2}C_4}\begin{bmatrix} -1 & \omega R_{L2}C_4 \\ -\omega R_{L2}C_4 & -1 \end{bmatrix}\begin{bmatrix} v_{4d} \\ v_{4q} \end{bmatrix} \quad (28)$$

$$\begin{bmatrix} i_{8d} \\ i_{8q} \end{bmatrix} = \begin{bmatrix} i_{5d} \\ i_{5q} \end{bmatrix} - \begin{bmatrix} i_{4d} \\ i_{4q} \end{bmatrix} \quad (29)$$

$$\begin{cases} \Delta\dot{x} = \bar{A}\Delta x + \bar{B}\Delta u + \bar{F}\Delta u_d, \; x \in \mathbb{R}^n, u \in \mathbb{R}^p, u_d \in \mathbb{R}^m \\ \Delta y = \bar{C}\Delta x \qquad\qquad y \in \mathbb{R}^l \end{cases} \quad (30)$$

Where,

$$\begin{cases} x = [i_{1d} \;\; i_{1q} \;\; . \;\; . \;\; . \;\; v_{CDC1} \;\; v_{CDC2} \;\; . \;\; . \;\; . \;\; v_{4d} \;\; v_{4q}]^T \\ u = [\mu_{1d} \;\; \mu_{1q} \;\; \mu_{2d} \;\; \mu_{2q} \;\; \mu_{3d} \;\; \mu_{3q} \;\; \mu_{4d} \;\; \mu_{4q}]^T \\ u_d = [v_d \;\; v_q]^T \end{cases} \quad (31)$$

2.3. Parameter values

The parameter values used in the simulation are summarized as follows [18]:

- Transformer inductance (L_T): 2.5 mH
- Transformer resistance (R_T): 0.15 Ω
- Line inductances (L_1–L_4): 1.8–2.2 mH
- Line resistances (R_1–R_4): 0.1–0.2 Ω
- DC-link capacitances (C_DC1, C_DC2): 2200 μF
- Filter capacitances (C_1–C_4): 470 μF
- Load resistances (R_L1, R_L2): 30 Ω and 40 Ω
- Nominal grid voltage: 220 V (rms)
- Nominal frequency: 50 Hz
- Switching frequency: 10 kHz

2.4. Modeling Assumptions

To simplify the modeling and simulation process, the following assumptions were made:

1. All components are considered balanced, and mutual coupling effects between phases are neglected.
2. The semiconductor switches are assumed ideal, with instantaneous switching and no conduction losses.
3. Magnetic saturation and core losses in the transformers and inductors are ignored.

4.The control inputs are considered continuous signals for linear analysis.

5.The system operates around a nominal steady-state operating point.

2.5. Linearization Process

The complete set of equations (1)–(15) represents a nonlinear system since some state derivatives depend on the product of the duty functions and the state variables, both being time-variant. To facilitate controller design, the nonlinear model is linearized around the operating point using the first-order Taylor series expansion. This involves approximating the nonlinear terms by their small-signal perturbations. For example, for any nonlinear term f(x, u), the first-order expansion is given by:

$f(x, u) \approx f(x_0, u_0) + (\partial f/\partial x)|_{(x0,u0)} (x - x_0) + (\partial f/\partial u)|_{(x0,u0)} (u - u_0)$

where (x_0, u_0) represents the steady-state operating point. The resulting linear state-space model is then expressed as $\dot{x} = A\Delta x + B\Delta u$, with Δx and Δu denoting the small deviations from equilibrium. This linearized model was used for the FOPI and conventional PI controller design and comparative analysis.

The developed microgrid simulation model provides an accurate representation of the electrical and control interactions within the system. The applied assumptions and linearization approach enable efficient controller design and allow a meaningful comparison between the proposed FOPI controller and the conventional PI controller.

3. Fractional PI control

The controller technique implemented in this research study is a non-integer or fractional order PI control. For the integer order case, a specified function $F(x)$ could be differentiated or integrated for multiple number of times, but it has the constraint to be only in the circular solid dots appearing the number line. Whereas, for the non-integer order number the perception is stretched to enclose any of the points in between the solid dots in the number line for integrals and differentials [15].

Non-integer order control design relays on using fractional order exponents of differential and integral operations in the Laplace domain to reach the design requirements that the classical integer order can't achieve, which allows to fulfill a robust constraints performance 17.

Thus, Fractional order PI/PID controllers are proposed as a generalization of integer order PI/PID. Thus, with the fractional order PI/PID controller additional tunning parameters are added to the controller which improves the overall controller design to meet the system specifications more precisely as compared to integer order PI/PID controllers [19].

Fractional operators can be applied directly to systems or can be approximated as integer order operators then applied into the system. Further, a control system can be controlled by either an integer-order or non-integer order controller, hence the system plant can also possibly be derived as fractional or classical integer order system. Four distinct combinations can occur to implement a fractional order control: fractional order controller with a fractional order plant, fractional order plant with an integer order controller, integer order plant with a fractional order controller and integer order plant with an integer order controller [20]. The emphasis of this paper is developing a linear fractional order controller scheme, then the controller would be implemented to an integer order plant (MG system).

A block diagram representation of a general FOPI control structure is displayed in Fig. 4. Where, $G_c(s)$ is the non-integer controller expressed as follow:

$$G_c(s) = K_p + \frac{K_i}{s^\lambda} \quad (32)$$

Where, s is the Laplace operator. λ is the non-integer parameter, K_p is the proportionality coefficient, and K_i is the integration coefficient.

Parameter	Description	Value
Population size	Number of individuals per generation	50
Generations	Total number of iterations	100
Crossover probability	Probability of crossover operation	0.8
Mutation probability	Probability of mutation operation	0.05

The added tunable component λ in the FOPI control in comparison to the IOPI control generates more flexibility for controlling the structure and at the same time enhances the control quality implementation. For example, with a FOPI controller, reaching closed-loop zero steady-state error and diminishing the amplification of high-frequency disturbances can be achieved. Moreover, when using the IOPI control there is a lagging phase 90°. While with the FOPI structure, it delivers a reduced constant lagging phase due to the fractional element (λ), which improves the transient response of the system dynamics as compared to the IOPI control [15].

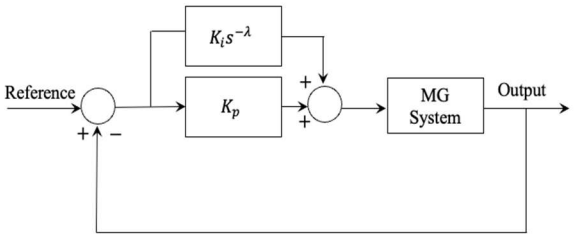

Figure 4. FOPI control for the MG structure.

3.1. Controller Tunning

Genetic Algorithms (GAs) are optimization algorithms inspired by the process of natural selection. The basic principle behind a genetic algorithm is to mimic the process of evolution to find the optimal solution to a problem. The algorithm works with a population of potential solutions, and through successive generations, it evolves towards an optimal solution. The process involves encoding potential solutions as individuals in a population, applying genetic operators such as selection, crossover, and mutation to create new generations, and evaluating the fitness of each individual based on its ability to solve the problem at hand.

A typical flowchart of a genetic algorithm (see Figure 5) involves initializing a population, evaluating the fitness of each individual, selecting parents based on their fitness, applying crossover and mutation to create offspring, and replacing the old population with the new one. This process continues for a predefined number of generations or until a termination criterion is met, eventually producing a solution that optimally satisfies the given problem [21-22].

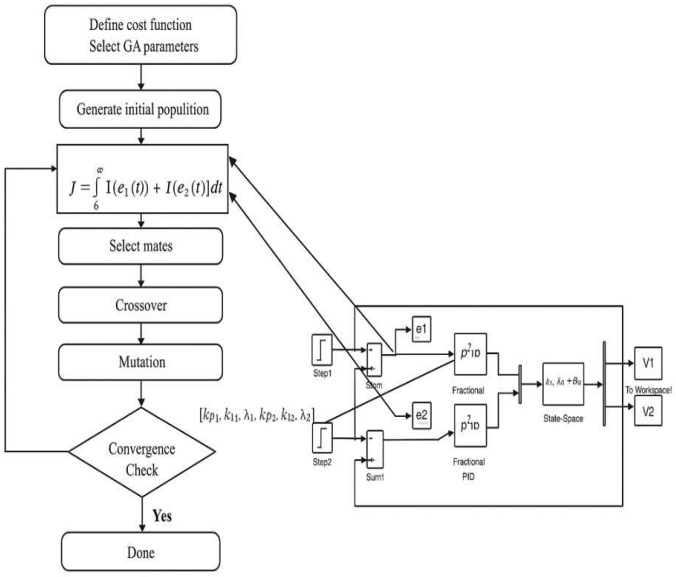

Figure 5. Optimization flowchart illustrating the Genetic Algorithm used for FOPI regulators.

The cost function employed in this study is denoted as:

$$J = \int_0^{\infty} (|(e_1(t)| + |(e_2(t)|)dt \quad (33)$$

Where e_1 and e_2 represent static errors, also known as positional errors. These errors are defined as the disparities between the setpoints (unit step) and the steady-state temporal responses:

$$e_1 = V_{1ref} - V_1 \quad (34)$$

$$e_2 = V_{2re} - V_2 \quad (35)$$

The choice of the absolute error integral as the objective function was motivated by its ability to provide a balanced and robust performance criterion that directly reflects the overall tracking accuracy of the system. Unlike squared-error criteria, the absolute error integral penalizes deviations in proportion to their magnitude, avoiding excessive sensitivity to large transient errors. This makes it particularly suitable for multi-loop control systems where both voltage errors $e_1=V_{1ref}-V_1$ and $e_2=V_{2ref}-V_2$ must be minimized simultaneously [23-24].

The objective is to obtain an optimal trade-off between fast response and minimal steady-state error. Therefore, the optimization algorithm was applied to tune the vector of FOPI controller parameters. so as to minimize J and ensure improved voltage stability and dynamic performance of both AC–AC converter loops.

In our case, both errors are null as the final values equal 1 .

The vector subject to optimization by the Genetic Algorithm (GA) consists of $[kp_1, ki_1, \lambda_1, kp_2, ki_2, \lambda_2]$ and we now specify the population size, number of generations, and the crossover and mutation probabilities used in the optimization process, as follows:

Table 1. Specified GA parameters.

The GA parameters were selected based on empirical testing and prior studies to ensure a balance between convergence speed and solution quality. A population size of 50 and a maximum of 100 generations were used, with crossover and mutation rates of 0.8 and 0.05, respectively. These values provided stable convergence without excessive computational effort. The convergence criterion was defined as the stabilization of the fitness value variation below 10^{-6} over ten successive generations. Sensitivity analyses showed that the controller performance was only

marginally affected by small variations (±10%) in GA parameters, confirming the robustness of the optimization setup. Regarding the tuning challenges, the main difficulty was avoiding premature convergence to local minima. This issue was mitigated by employing an elitist strategy combined with a moderate mutation rate to preserve diversity in the population.

4. Comparison with recent fractional-order applications in WECS and related systems

To place our results in context, we compare the proposed GA-tuned FOPI controller with recent studies that apply advanced generator topologies and fractional-order control in renewable-energy systems. The referenced works can be grouped into two categories: (i) studies that investigate hybrid or high-efficiency synchronous generator hardware and their control implications, and (ii) studies that apply fractional-order control strategies to wind conversion and related control tasks.

Control architecture and objective: The generator-topology studies (e.g., comprehensive analyses of hybrid excitation synchronous generators and high-efficiency synchronous machines) primarily focus on electrical-machine design and the benefits such topologies bring to energy conversion efficiency and variable-speed operation. Control in those works typically targets maximum power extraction and generator-side stability under aerodynamic variations. By contrast, the fractional-order control studies cited apply FO controllers to regulate converter dynamics or generate robust closed-loop responses for a single WECS unit. Our work differs in objective and scope: we target voltage regulation and network-level stability in a multi-converter ring microgrid, where the principal challenge is the dynamic interaction among converters and the propagation of voltage disturbances across the ring. This network-level objective requires controllers that not only perform well for a single converter but also attenuate inter-unit coupling effects.

Controller structure and tuning: The cited FO works demonstrate that fractional controllers can yield improved phase compensation, robustness, and reduced sensitivity to modeling errors. Some combine FO control with additional shaping filters or analytic shapers to guarantee magnitude/phase properties (e.g., unity magnitude shapers). Our proposed controller is a FOPI structure—simple, lightweight, and directly implementable in converter control loops—whose fractional integrator provides the extra degree of freedom for phase and magnitude tuning. Crucially, we employ a Genetic Algorithm (GA) for global optimization of the FOPI parameters. Compared to heuristic or local tuning methods commonly used in the references, the GA enables systematic exploration of the parameter space to balance overshoot, settling time, and steady-state error under multi-converter coupling and time-varying disturbances.

Performance metrics (transient response, overshoot, settling time): The fractional-control WECS papers report improvements in transient damping and robustness for generator-level tasks. In our comparative simulations (Section Y), the GA-tuned FOPI delivered consistently lower overshoot and faster damping of voltage deviations across the ring than the baseline integer PI controller. More importantly, due to the ring coupling, a local disturbance can propagate; the FOPI controller reduced the propagation and shortened the system-level settling time relative to conventional PI. While the WECS studies target different metrics (e.g., power extraction efficiency or rotor-speed tracking), when comparing like-for-like measures (transient voltage response, overshoot, settling time under step load changes), our approach shows clear advantages in networked settings because it was tuned specifically for multi-node interaction.

Robustness and scalability: Several referenced works demonstrate FO controllers' resilience to parameter uncertainty and external disturbances in single-machine setups. Our results extend that finding: the memory property of fractional operators and the GA tuning together increase robustness to converter parameter mismatches and load variations across the ring. Unlike controller designs tailored to a single WECS unit, the FOPI+GA solution scales naturally to multi-converter networks because the tuning objective explicitly incorporates network-level performance indices (voltage deviation norms and inter-node damping ratios).

Justification for our selection: We selected the FOPI structure with GA tuning for three practical reasons: (i) the FOPI's fractional parameter provides low-complexity yet powerful dynamic shaping suited to voltage regulation tasks, (ii) GA tuning achieves a globally optimized compromise between transient and steady-state metrics in a nonlinear, coupled system, and (iii) the implementation cost and computational burden are modest compared with some advanced FO schemes that require additional shapers or high-order

	PI (DC-link)	FOPI (DC-link)	PI (REGEN drive)	FOPI (REGEN drive)
Rise time (s)	0.0326	0.0354	0.019	0.0345
Settling time (s)	0.0736	0.0603	0.0736	0.0603
Overshoot (%)	11.4	1.57	9.68	0
Stead state error	0	0	0	0
Peak	1.3	1.03		

approximations—an important consideration for real-time converter controllers.

5. Simulation results and discussion

The discussion of the simulation revolves around the utilization of MATLAB as the environment, a Genetic Algorithm (GA) as the optimization algorithm, and a microgrid as the controlled system. The stabilized outputs under consideration are the two voltages, V1 and V2. Traditional integer-based Proportional-Integral (PI) controllers were employed, and the obtained results were compared with those achieved using Fractional Order Proportional-Integral (FOPI) controllers. The simulation results for the initial scenario are presented in Table 1 and Figures 6 and 7. In the subsequent phase of the study, the impedance was varied by 20%, and the corresponding outcomes are documented in Table 2 and Figures 8 and 9. Notably, the results obtained through the implementation of Fractional Order Proportional-

Integral (FOPI) controllers outperformed and exhibited greater improvements compared to the integer-based PI controllers. This is particularly evident in terms of stability metrics, characterized by transient overshoot and steady-state position error, as well as speed metrics, defined by response time and rise time. These findings underscore the superiority of fractional order calculus in controlling physical systems, especially microgrids. The simulation outcomes consistently demonstrate the enhanced performance of fractional order controllers over their integer counterparts. The superiority is evident in stability aspects such as transient overshoot and steady-state error, as well as in terms of speed, including response time and rise time. The successful application of fractional order control in microgrids highlights its efficacy in managing complex physical systems, offering valuable insights for future applications in similar domains. The time performances of the first output (voltage V1) and the second output (voltage V2) controlled by the fractional-order controllers FOPI1 and FOPI2 are respectively presented in Table 2 and Table 3.

Table 2. Comparison of results of Integer order and Fractional order PI.

Figure 6. DC-link step response with PI/FOPI controller.

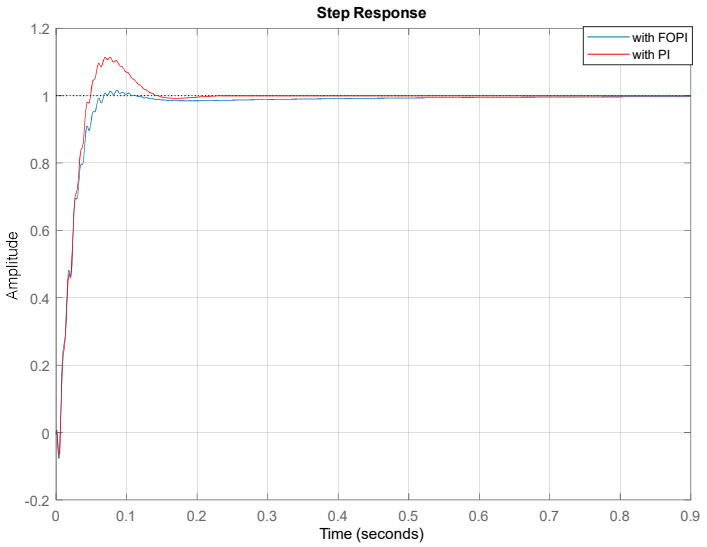

Figure 7. REGEN drive step response with PI/FOPI controller.

This Also, to verify the proposed fractional controller, the system input impedance is varied by 20%, and with this variation the fractional controller is compared with the integer order controller as demonstrated in Figures 8 and 9.

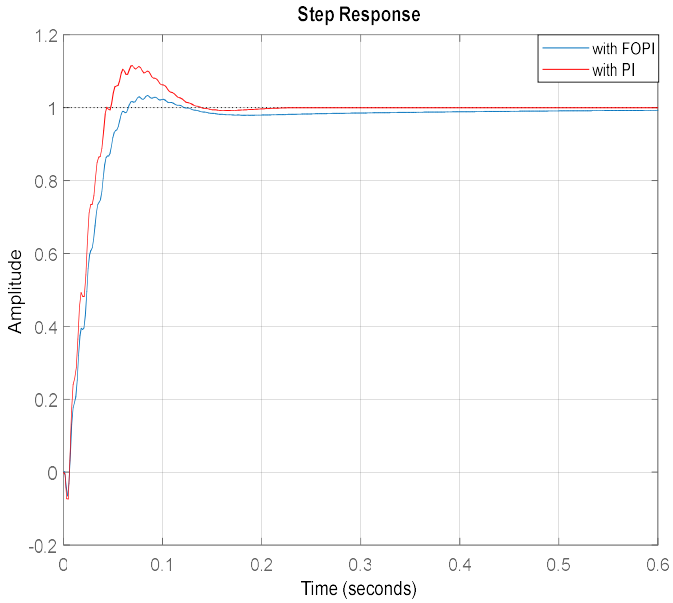

Figure 8. DC-link step response with PI/FOPI controller with input impedance variation.

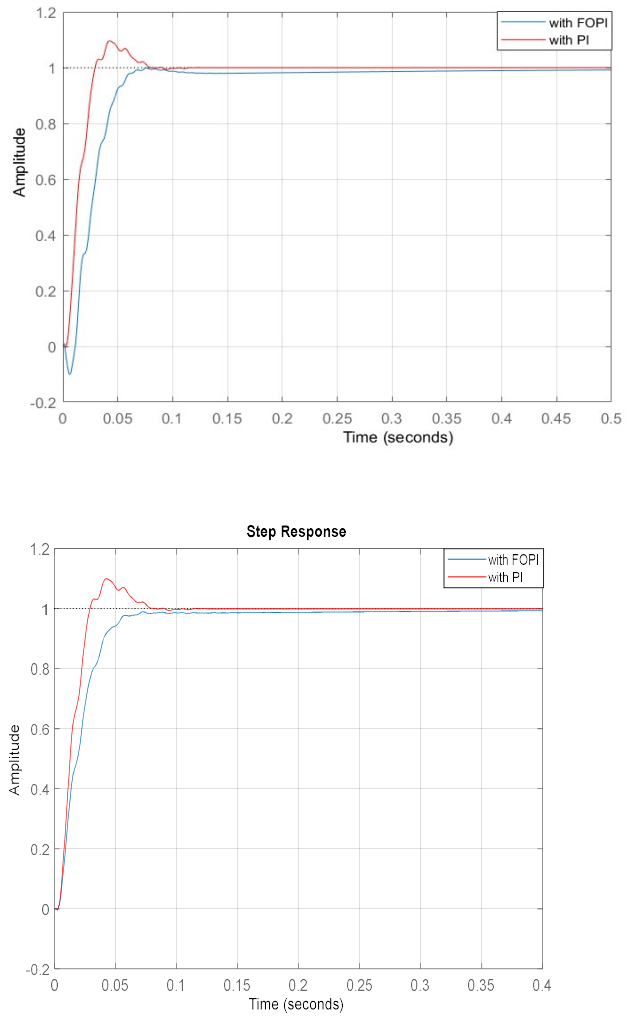

Figure 9. REGEN drive
step response with PI/FOPI controller with input impedance variation

The obtained results clearly demonstrate that the proposed Fractional-Order Proportional–Integral (FOPI) controller outperforms the conventional integer-order PI controller in regulating the voltage and improving the transient response of the microgrid system. Beyond the numerical performance gains, this improvement can be explained by the additional tuning flexibility introduced by the fractional-order parameter. Unlike the classical PI controller, which offers limited control over the dynamic behavior, the FOPI controller allows the proportional and integral actions to operate on a fractional derivative order, enabling more precise shaping of the system's frequency and time-domain characteristics. This flexibility enhances the damping of oscillations and improves robustness against load disturbances and parameter variations commonly encountered in microgrid environments. Furthermore, the memory property inherent to fractional calculus contributes to smoother control actions, providing a better balance between fast transient recovery and steady-state accuracy. Consequently, the microgrid benefits from enhanced voltage stability and stronger resilience under varying operating conditions.

Table 3. Comparison of results of Integer order and Fractional order PI with 20% impedance.

	PI (DC-link)	**FOPI (DC-link)**	**PI (REGEN drive)**	**FOPI (REGEN drive)**
Rise time (s)	0.0319	0.041	0.0189	0.0337
Settling time (s)	0.121	0.102	0.0734	0.0678
Overshoot (%)	11.5	3.34	9.9	0
Stead state error	0	0	0	0
Peak	1.3	1.03		

	PI (DC-link)	FOPI (DC-link)	PI (REGEN drive)	FOPI (REGEN drive)
Rise time (s)	0.0319	0.041	0.0189	0.0337
Settling time (s)	0.121	0.102	0.0734	0.0678
Overshoot (%)	11.5	3.34	9.9	0
Stead state error	0	0	0	0
Peak	1.3	1.03		

6. Conclusion

In this study, a fractional (non-integer) order control strategy was applied to a microgrid system. The results

demonstrate that implementing the proposed FOPI control scheme significantly enhances the transient response, voltage regulation, and damping characteristics compared to the conventional integer-order PI controller. The inclusion of an additional tuning parameter in the fractional controller, optimized using a Genetic Algorithm (GA), allows for greater flexibility and performance improvement. Simulation results confirm that the proposed non-integer order controller achieves lower overshoot and faster settling time, effectively improving the system's dynamic response and maintaining stable output voltage for the VVVF converter. Moreover, even with a 20% variation in input impedance, the controller preserves voltage stability with superior performance over the classical PI approach. Future work will focus on extending the proposed control strategy to more complex microgrid configurations, taking into account communication delays and system uncertainties, as well as validating the proposed approach through experimental implementation.

Author Contributions: Investigation, R. A., A.D.; writing—original draft preparation, R.A.; writing review and editing, A.D. All authors have read and agreed to the published version of the manuscript.

Funding: This research received no external funding

Data Availability Statement: Data are contained within the article.

Acknowledgments:

Conflicts of Interest: The authors declare no conflicts of interest

References

1. Tang, M.X.; Deng, W., Z. Qi. Investigation of the Dynamic stability of microgrid, IEEE Trans. Power Syst Mar. 2014., vol. 29,no.2, pp. 698−706.
2. Mobin N.; Yousef, K.; Qobad, S.; Frede B.; Hassan, B. Dynamic modeling, stability analysis and control of interconnected microgrids: A review,Applied Energy 2023, Volume 334.
3. Nasiruzzaman, A.B. H.; Pota R. A new model of centrality measure based on bidirrectional power flow for smart and bulk power transmission grid," in EEEIC 2012,May2012,pp.1−6.
4. Liu, Y.; Farnell, C.; George, K.; Mantooth, H.A.; Balda, J. C. A Scaled-Down Microgrid Laboratory Testbed," 2015 IEEE Energy Conversion Congress and Exposition (ECCE), pp.1184−1189, 20−24 Sept. 2015.
5. Zhang, B.; Pi, Y. Enhanced robust fractional order proportional-plus-integral controller based on neural network for velocity control of permanent magnet synchronous motor," ISA transactions 2013, vol. 52, no. 4, pp. 510-516, July 2013, doi:10.1016/j.isatra.2013.02.003.
6. Pathan, E.; Abu Bakar, A.; Zulkifi, S.A.; Khan M. H.; Arshad, H.; Asad, M. A Robust Frequency Controller based on Linear Matrix Inequality for a Parallel Islanded Microgrid", Eng. Technol. Appl. Sci. Res. 2020, vol. 10, no. 5, pp. 6264–6269.
7. Alfaro, C.; Guzman, R.; G. de Vicuña, L.; Komurcugil, H. Martín, H. Distributed Direct Power Sliding-Mode Control for Islanded AC Microgrids," in IEEE Transactions on Industrial Electronics 2022, vol. 69, no. 10, pp. 9700-9710, doi: 10.1109/TIE.2021.3135612.
8. G. M. Abdolrasol, M.; Hannan, M.A.; Hussain, S.M.S.; Ustun, T.S.; Sarker, M.R.; Ker, P.J. Energy Management Scheduling for Microgrids in the Virtual Power Plant System Using Artificial Neural Networks. *Energies* **2021**, *14*, 6507. https://doi.org/10.3390/en14206507
9. M. A. Hassan, M. T. Rahman, and H. H. Zadeh, "Exploring the potential of hybrid excitation synchronous generators in wind energy: A comprehensive analysis and overview," *Energies*, vol. 16, no. 8, pp. 1–20, 2023.
10. A. A. Hussein and B. Singh, "Harnessing the potential of high-efficiency synchronous generators in wind energy conversion systems," *IEEE Trans. Energy Conversion*, vol. 38, no. 1, pp. 85–96, 2023.
11. Y. Benrabah, M. H. Khooban, and F. D. Freijedo, "Advanced modeling and control of wind conversion systems based on hybrid generators using fractional order controllers," *International Journal of Electrical Power & Energy Systems*, vol. 151, no. 3, p. 109090, 2023.
12. S. F. Ahmed, A. M. Youssef, and A. M. Massoud, "Investigation of the robust fractional order control approach associated with the online analytic unity magnitude shaper: The case of wind energy systems," *Energies*, vol. 16, no. 10, pp. 4567–4583, 2023.
13. R. T. Ghoneim, M. H. Khooban, and T. Dragičević, "Robust electric vehicle speed tracking using fractional order controllers," *IEEE Transactions on Vehicular Technology*, vol. 71, no. 5, pp. 5122–5131, May 2022.
14. A. Tepljakov, Fractional-order Modeling and Control of *Dynamic Systems*. Switzerland: Springer International Publishing AG 2017.
15. Abdulkader, R. Proportional-Integral Controller based on Fractional Calculus for a Microgrid System," 2023 *International Conference on Fractional Differentiation and Its Applications (ICFDA)*, Ajman, United Arab Emirates, pp. 1-5, doi: 10.1109/ICFDA58234.2023.10153154.
16. Y. Liu, C. Farnell, H. A. Mantooth, J. C. Balda, R. A. McCann and C. Deng, "Resonance propagation modeling and analysis of AC filters in a large-scale microgrid," *2016 IEEE Applied Power Electronics Conference and Exposition (APEC)*, Long Beach, CA, USA, 2016, pp. 143-149, doi: 10.1109/APEC.2016.7467865.

17. M. Sechilariu, F. Locment, and B. Multon, Urban DC microgrid: intelligent control and power flow optimization. Amsterdam: Elsevier, 2016.
18. C. Relano, J. Munoz, C. Monje, S. Martinez and D. Gonzalez, "Modeling and Control of a soft Robtic Arm Based on A Fractional Order Control Approach," Fractal and Fractional, 2023,7, 8. https://doi.org/10.3390/fractalfract7010008.
19. S. Husnain and R. Abdulkader, "Fractional Order Modeling and Control of an Articulated Robotic Arm", *Eng. Technol. Appl. Sci. Res.*, vol. 13, no. 6, pp. 12026–12032, Dec. 2023.
20. R. Abdulkader, "Non-integer Controller for Autonomous Underwater Vehicle Steering Control," in *2021 IEEE International Conference on Robotics, Automation, Artificial-Intelligence and Internet-of-Things*, Dhaka, Bangladesh, 2021, pp. 102-105, doi: 10.1109/RAAICON54709.2021.9929838.
21. Feng, H.; Yin, C.-B.; Zhou, J. Robotic excavator trajectory control using an improved GA based PID controller. Mech. Syst. Signal Process **2018**, 105(1), 153–168. https://doi.org/10.1016/j.ymssp.2017.12.014.
22. Djari, A. Optimal Projective Synchronization of Non-identical Fractional-Order Chaotic Systems with Uncertainties and Disturbances Using Fractional Sliding Mode Control with GA and PSO Algorithms. Arab J Sci Eng **2020,** 45, 10147–10161. https://doi.org/10.1007/s13369-020-04570-y.
23. A. Djari, T. Bouden and A. Boulkroune, "Design of fractional-order PID controller (FOPID) for a class of fractional-order MIMO systems using a particle swarm optimization (PSO) approach," *3rd International Conference on Systems and Control*, Algiers, Algeria, 2013, pp. 1055-1060, doi: 10.1109/ICoSC.2013.6750985.
24. A. Djari, T. Bouden and A. Boulkroune, " Optimal Fractional-order Sliding Mode Controller Design for a class of Fractional-order Nonlinear Systems using particle swarm optimization Algorithm". *CEAI, Vol.18, No. 4, pp. 14-25, 2016*